*33rd EPS Conference on Plasma Phys. Rome, 19 - 23 June 2006 ECA Vol.**30I**, P-4.197 (2006)*

Optimizing Compact Stellarator Performance

J. F. Lyon[1], L.P. Ku[2], L. El-Guebaly[3], L. Bromberg[4] and the ARIES Team

[1] *Oak Ridge National Laboratory, PO Box 2008, MS-6169, Oak Ridge, TN 37831, USA*

[2] *Princeton Plasma Physics Laboratory, PO Box 451, Princeton, NJ, 08543-0451, USA*

[3] *University of Wisconsin, 1500 Engineering Drive, Madison, WI, 53706-1687, USA*

[4] *Massachusetts Inst. of Technology, 167 Albany St., Cambridge, MA, 02139, USA*

Abstract. Building on the NCSX and QPS experiments, compact stellarator parameters are optimized for large, next-generation experiments and fusion power plants.

1. Compact Stellarator Configurations. Compact stellarators are a new type of toroidal magnetic configuration that features: (1) quasi-symmetry that leads to low viscosity and large flows that can break apart turbulent eddies and reduce anomalous transport; (2) low effective helical field ripple that leads to low neoclassical transport; (3) low plasma aspect ratio that leads to larger plasma radius for a given major radius and cost; (4) use of a small bootstrap current to supplement the rotational transform from the external nonplanar coils; and (5) higher instability limits and robust magnetic surfaces that allow higher beta operation.

Two compact stellarator experiments have been designed to test complementary optimization principles: quasi-axisymmetry in the National Compact Stellarator Experiment (NCSX, now under construction) and quasi-poloidal symmetry in the Quasi-Poloidal Stellarator Experiment (QPS, now in the R&D and prototype development stage). NCSX has a magnetic configuration similar to that of a tokamak with globally reversed shear and plasma aspect ratio $\langle R\rangle/\langle a\rangle$ = 4.4. QPS has a magnetic configuration similar to that of toroidally linked mirrors with rotational transform ι and $\langle R\rangle/\langle a\rangle$ = 2.7. These experiments have V_{plasma} ~ 2–3 m^3, an average on-axis field $\langle B\rangle$ ~ 1–2 T, pulse lengths ~ 0.2–1 s and P_{heating} ~ 3–6 MW.

2. Optimization of Next-Generation Experiments. The next step in development of the compact stellarator approach is to scale these configurations to larger plasma size, magnetic field and heating power, comparable to the values for the present large tokamaks: V_{plasma} ~ 30–60 m^3, $\langle B\rangle$ ~ 3–4 T, pulse lengths ~ 1 hour and P_{heating} ~ 30 MW. Physics targets are $T_{\text{e,i}}$ ~ 10 keV and $\langle\beta\rangle$ ~ 5%. Cost minimization is an important criterion for a large device and superconducting coils are needed rather than copper coils. Plasma performance can be estimated using a confinement multiplier H^{ISS95} for the 1995 international stellarator scaling relation $\tau_E^{ISS\text{-}95} = 0.079\, a^{2.21} R^{0.65} P^{-0.59} n^{0.51} B^{0.83} \iota^{0.4}$.

Figure 1 illustrates the integrated plasma and coil optimization procedure used in developing

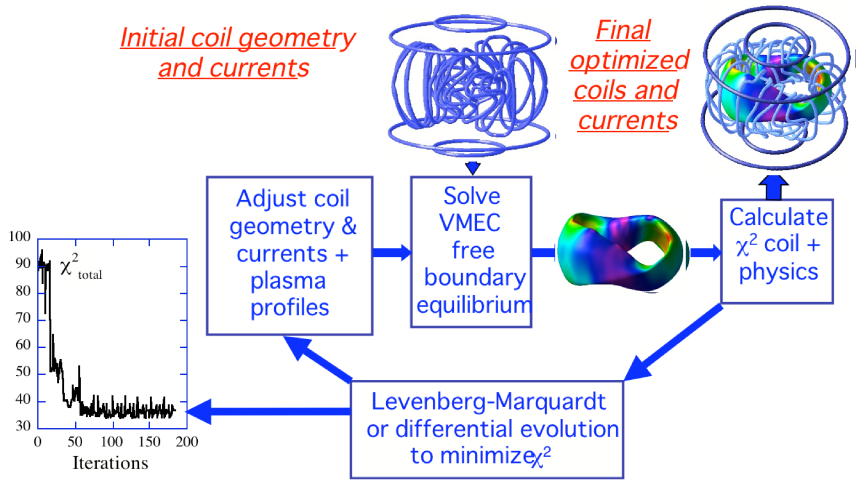

Fig. 1. Plasma and coil optimization procedure.

compact stellarator configurations. The optimization targets include those for:
(1) plasma geometry (aspect ratio, average ellipticity, surface curvature and radial centering),
(2) coil geometry (plasma-coil distance, coil-coil separation, coil-coil distance across the center, coil curvature, maximum radial extent, and poloidal coil current), and
(3) magnetic configuration (the desired Fourier harmonics of $|\mathbf{B}|$, $\iota(r)$ and bounds, edge shear, maximum plasma current, bootstrap current, parallel current on low-order resonant surfaces, $\langle\beta\rangle$, ballooning mode stability, Mercier stability, B_{normal} residue in the vacuum configuration, and $\varepsilon^{3/2}$ -- the coefficient of the $1/\nu$ neoclassical transport at low collisionality without the ambipolar electric field). Typically ~200 Fourier harmonics are used to describe the shape of the non-axisymmetric plasma surface and the coil geometry.

Figures 2 – 5 show the effect of varying the average major radius $\langle R\rangle$, $\langle B\rangle$, average plasma density n and H^{ISS95} from the reference values $\langle R\rangle$ = 2.25 m, $\langle B\rangle$ = 3 T, n = 3 x 10^{20} m^{-3} and H^{ISS95} = 3 for the QPS plasma configuration (aspect ratio 2.7) with $P_{heating}$ = 30 MW. The red diamonds indicate the reference value. The other values for the main reference device and plasma parameters are average plasma radius $\langle a\rangle$ = 0.83 m, V_{pl} = 31 m^3, energy confinement time τ_E = 0.33 s, central temperature T_0 = 6.8 keV, $\langle\beta\rangle$ = 6.1%, plasma energy W_{pl} = 10 MJ and $Tn\tau_E$ = 6.8 x 10^{20} keV-m^{-3}-s. These parameters are sufficient for demonstrating large-tokamak-level performance in compact stellarators. Larger values for R and B would lead to a more expensive device since cost is roughly proportional to R^2B. The "Sudo" density "limit" based on Heliotron-E data is 1.9 x 10^{20} m^{-3} (values 2–3 x n_{Sudo} are now obtained in the LHD experiment), so higher density operation should be possible, which leads to higher τ_E, $\langle\beta\rangle$, W_{pl} and $Tn\tau_E$. Present experiments obtain H^{ISS95} values of 2–2.5, but the 2004 update of the stellarator confinement scaling suggest an $\varepsilon_{eff}^{-0.4}$ dependence, which should give higher values

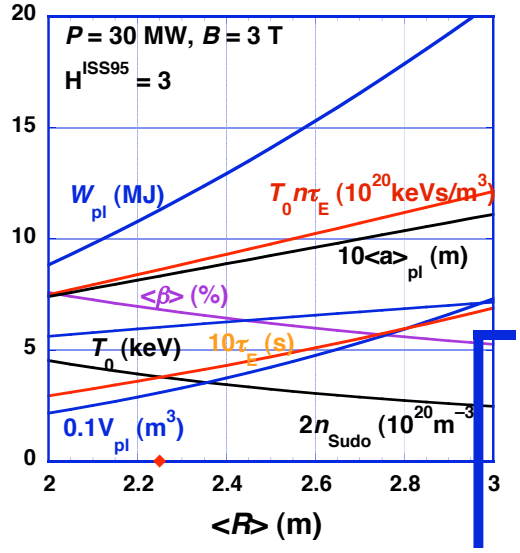

Fig. 2. Parameter variation with ⟨R⟩.

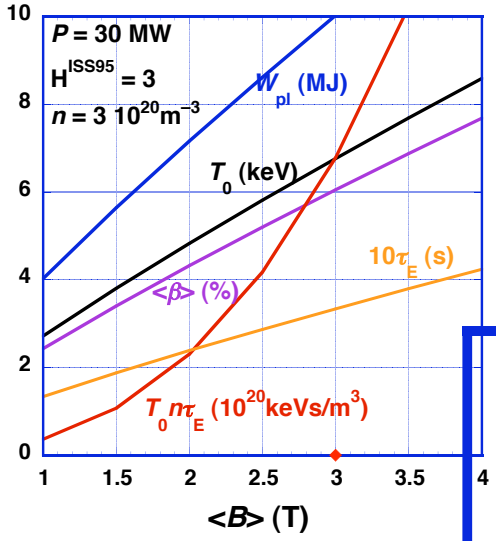

Fig. 3. Parameter variation with <B>.

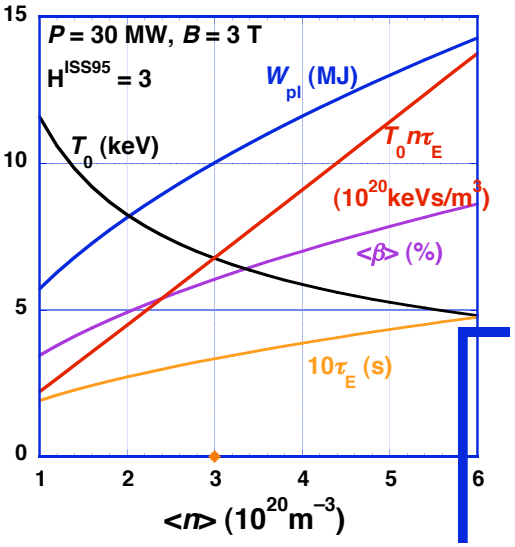

Fig. 4. Parameter variation with n.

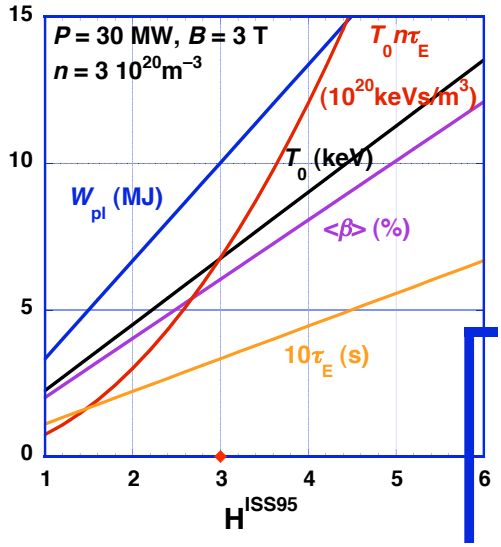

Fig. 5. Parameter variation with H^{ISS95}.

for H^{ISS95} than in present experiments because of the reduced ε_{eff} in compact stellarators, and hence higher plasma parameters.

3. Optimization of Compact Stellarator Reactors.

The need to shield the superconducting coils from neutrons and to breed tritium introduces a new set of optimization criteria and constraints. Compact stellarator power plants require a large scaleup in device parameters: V_{plasma} ~ 400–500 m^3, $\langle B \rangle$ ~ 5-6 T and true steady-state operation, but only $P_{heating}$ ~ 20 MW to ignite. Figure 6 shows one of the compact stellarator configurations analyzed: a 3-field-NCSX-based plasma with coils modified to allow

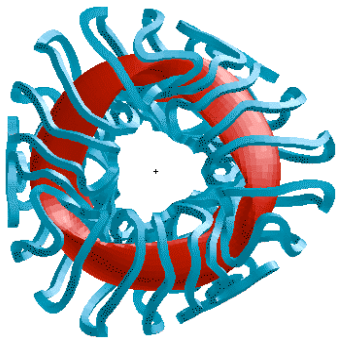

Fig. 6. NCSX-like plasma and coils.

larger plasma-coil spacing, improved confinement of energetic particles, and an enhanced mirror term. A 1-D systems code that incorporates a nonlinear constrained optimizer was used to examine the effect of transport models, the variation of density and temperature profiles, large radiation losses, impurity and helium accumulation, $\langle\beta\rangle$ limits, energetic particle losses, and constraints needed for a practical device including plasma-coil spacings, coil-coil spacings, allowable power densities on plasma-facing components and the divertor, and the maximum allowable field on the Nb_3Sn superconducting coils.

Figure 7 shows values for $\langle R\rangle$, $\langle R\rangle/\langle a\rangle$, and the plasma cross section for the ARIES-AT and ARIES-RS power plants and the most recent stellarator reactor studies, indicating that compact stellarator power plants can be comparable in size with tokamaks. Table I gives the parameters for an NCSX-based reference case. The 7.75-m value for $\langle R\rangle$ was chosen to meet a number of constraints: adequate space between the plasma surface and the center of the coils for the plasma scrapeoff distance, tritium breeding blanket, shielding, manifolds, vacuum vessel, inner coil structure and half the winding pack; maximum neutron wall loading <4.5 MW/m^2; and a tritium breeding ratio >1.1 with an adequate margin on the fraction of ^{6}Li in the blanket. A tapered blanket was used to take advantage of the fact that the plasma is close to the coils only over a small fraction of the first wall area (Fig. 8). 75% of the power in the core and in the scrapeoff layer is radiated, allowing for the power peaking on the divertor.

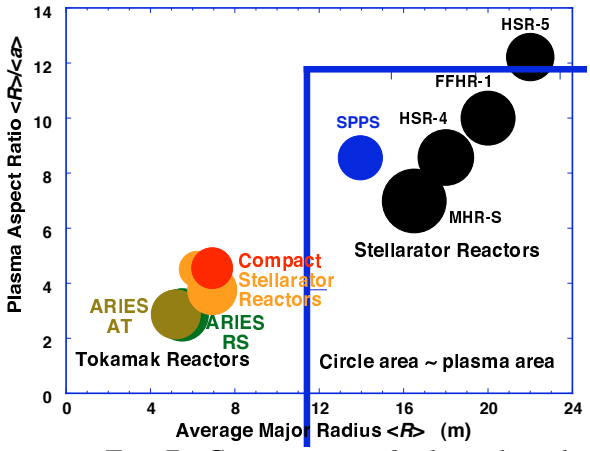

Fig. 7. Comparison of tokamak and stellarator power plants

$\langle R\rangle$ (m)	7.75	COE	79.0
$\langle B_{axis}\rangle$ (T)	5.70	P_{fusion} (MW)	2364
$\langle n\rangle$ 10^{20}m^{-3}	3.58	TBR	1.115
$\langle T\rangle$ (keV)	5.73	τ_E (s)	0.96
H-ISS95	1.48	% P_{rad}	75.0
$f_{\alpha,loss}$ %	5	$f_{rad,SOL}$ %	75
% Fe	0.008	P_{rad} (MW)	354
$p_{n,max}$ MW/m^2	3.95	P_{cond} (MW)	94.4
$n/2n_{Sudo}$	0.94	P_{div} (MW)	108
B_{max} (T)	15.08	P_{wall} (MW)	364

Table I. Parameters for a reference case.

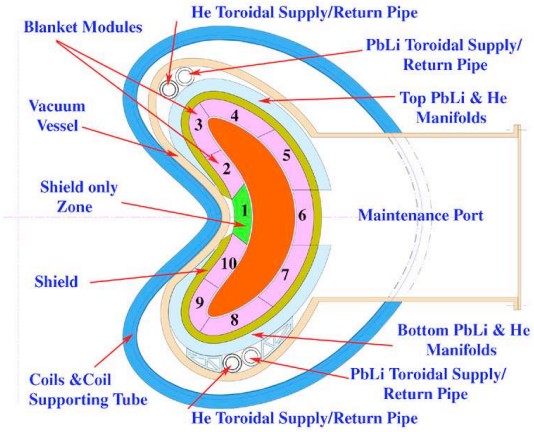

Fig. 8. Cross section of the power plant core.

Supported by USDOE under Contract DE-AC05-00OR22725 with UT-Battelle, LLC.